Letter

# Optimization of current-based sensing of phonon temperature using a finite reservoir

Sindre Brattegard,[1,*] Stephanie Matern,[2,†] Mark T. Mitchison,[1,3,‡] and Saulo V. Moreira[1,§]
[1]*School of Physics, Trinity College Dublin, College Green, Dublin 2, Ireland*
[2]*Pitaevskii BEC Center, CNR-INO and Dipartimento di Fisica, Università di Trento, 38123 Trento, Italy*
[3]*Department of Physics, King's College London, Strand, London WC2R 2LS, United Kingdom*

(Received 15 May 2026; revised 15 September 2026; accepted 14 October 2026; published 9 November 2026)

In realistic nanoscale transport setups, electron-phonon coupling leads to the exchange of heat between phonon baths and electronic reservoirs with finite heat capacities. Such exchange affects the finite reservoir's temperature. However, this sensitivity of the finite reservoir temperature to the exchange of heat with the finite reservoir has remained unexplored for thermometry. Here, we fill this gap by combining current metrology techniques with a thermodynamic framework encompassing finite reservoirs. We focus on an experimentally realizable setup with a quantum dot coupled to a finite reservoir and consider two distinct current-based strategies in the long-time limit, namely monitoring quanta exchanged between the quantum dot and finite reservoir and the measurement of the total current flowing from the quantum dot into an infinite reservoir. A third strategy involves measurements of the quantum dot occupation. For a large but finite reservoir, we show that the Fisher information for all three strategies captures the finite reservoir's contribution to sensitivity through common factors. We also demonstrate that monitoring quanta exchanged between the system and finite reservoir in the long-time limit achieves optimal precision. Finally, we provide an optimization analysis that explores how maximal precision can be achieved within each of the current-based strategies by tuning the gate voltage.

DOI: 10.1103/7jl4-jryx

*Introduction*. Measuring the temperature of phonons is fundamental for understanding thermoelectric properties influencing the performance of quantum electronic devices. Devising practical high-precision phonon temperature measurements is, nonetheless, challenging. In experiments, the phonon temperature is often inferred using spectroscopic methods, in particular Raman spectroscopy [1,2]. While commonplace, Raman thermometry techniques have relatively low precision and can be sensitive to imperfections in the sample [3].

In nonequilibrium experimental configurations, heat exchanges between electron and phonon reservoirs enabled by electron-phonon coupling carry information about the phonon bath's parameters. Focusing on measurements of transport observables, such as currents, could, therefore, potentially lead to advantageous estimation schemes. Most importantly, current observables are experimentally accessible in a variety of open-system platforms at the nanoscale.

In this vein, current-measurement-based parameter estimation strategies recently started to gain traction. Examples include measuring currents for the estimation of system or environment parameters in nonequilibrium scenarios, such as thermometry exploiting quantum thermal machines [4] and quantum dot (QD) setups [5,6]. Further recent theoretical advances include the derivation of classical and quantum parameter estimation bounds in mesoscopic electronic settings employing an adiabatic linear-response approach [7] and the Landauer-Büttiker formalism [8]. As well as this, Bayesian approaches for continuously measured two-level systems coupled to fermionic or bosonic environments have been investigated [9].

Previous works on current-based metrology have approximated the environments driving the system out of equilibrium as being infinitely large. Notably, however, many realistic experimental transport setups encompass finite-size reservoirs [10–14], which undergo fast internal thermalization due to electron-electron interactions [15,16]. Due to its finite heat capacity, the temperature of such a finite reservoir is affected by exchanges of heat with the surroundings. This feature has been shown to influence transport properties [17–21], nonequilibrium thermodynamics [22–26], and heat-engine performance [27–29], but it also makes finite reservoirs ideal platforms for calorimetry [30]. Indeed, recent experiments have demonstrated electronic nanocalorimeters that can detect tiny amounts of heat exchange via measurable changes in their temperature [31,32]. This sensitive relationship between heat exchange and temperature naturally suggests that finite reservoirs could also be exploited for current-based thermometry, yet to date this possibility has remained unexplored in the literature.

In this Letter, we investigate phonon temperature estimation by combining current-based metrology techniques with transport theory encompassing finite-size reservoirs. We focus

*Contact author: brattegs@tcd.ie
†Contact author: materns01@gmail.com
‡Contact author: mark.mitchison@kcl.ac.uk
§Contact author: moreirsv@tcd.ie

*Published by the American Physical Society under the terms of the Creative Commons Attribution 4.0 International license. Further distribution of this work must maintain attribution to the author(s) and the published article's title, journal citation, and DOI.*

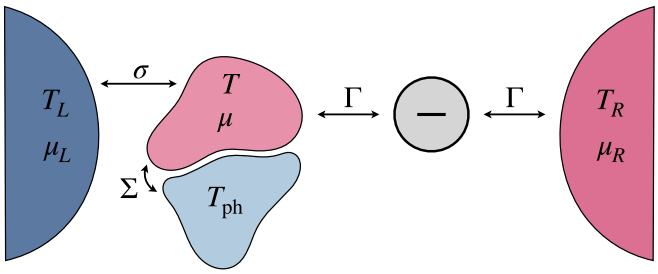



FIG. 1. Sketch of the finite-size reservoir at stationary temperature and chemical potential, $T$ and $\mu$, coupled to a phonon bath at temperature $T_{\rm ph}$ and to the quantum dot system. The finite reservoir is also coupled to the left infinite-size reservoir at temperature $T_L$ and $\mu_L$, while the quantum dot is coupled to another infinite-size reservoir to its right, at temperature $T_R$ and chemical potential $\mu_R$.

on an experimentally realizable nonequilibrium transport setup supporting particle and heat currents, where an electronic finite reservoir is both coupled to a bath of phonons and a single-level QD. Our analysis considers two distinct current-measurement-based strategies in the long-time limit: (I) monitoring quanta exchanged between the QD and the baths, and (II) measuring the net particle current going through the QD into an infinite reservoir. Pivoting from current measurements, we consider a third strategy, i.e., (III) measuring the QD occupation. We derive analytical expressions for the Fisher information for these three strategies under the assumption of a large, but still finite, reservoir. All three formulas are shown to share factors revealing how finite reservoirs can be harnessed for thermometry. Furthermore, while we show that strategy I enables the optimal performance achievable in our setup, our optimization analysis further explores how maximal precision can be achieved by tuning the gate voltage within each current-based strategy (I and II).

*Nonequilibrium transport setup*. We consider the setup sketched in Fig. 1, where the electronic finite reservoir QD is coupled to left (L) and right (R) infinite-size reservoirs at different temperatures $T_{L/R}$ and chemical potentials $\mu_{L/R}$. Furthermore, the finite reservoir exchanges heat with a bath of phonons at some temperature $T_{\rm ph}$ as depicted in Fig. 1. We take all electronic reservoirs to consist of noninteracting electrons, described by Fermi-Dirac distributions $f(E,\tilde{T},\tilde{\mu}) = [1+e^{(E-\tilde{\mu})/\tilde{T}}]^{-1}$ (we set $k_B = 1$). The finite reservoir's thermalization via electron-electron interaction is considered to be very fast, so that it is in a quasiequilibrium state at all times, with well-defined, time-dependent temperature $T(t)$ and chemical potential $\mu(t)$, characterized by $f(E,T(t),\mu(t))$ [32,33].

The time evolution of the system is described by the following phenomenological master equation [34],

$$\frac{d}{dt}\begin{bmatrix}p_0\\p_1\end{bmatrix} = \mathcal{W}\begin{bmatrix}p_0\\p_1\end{bmatrix} = \sum_{\alpha=L,R}\begin{bmatrix}-\Gamma_\alpha^{\rm in} & \Gamma_\alpha^{\rm out}\\ \Gamma_\alpha^{\rm in} & -\Gamma_\alpha^{\rm out}\end{bmatrix}\begin{bmatrix}p_0\\p_1\end{bmatrix}, \quad (1)$$

where $p_n$ denotes the probability of the QD being in state $n = \{0,1\}$, i.e., empty ($n=0$) or occupied ($n=1$). The tunneling rates for electrons to jump in or out of the QD are given by [35]

$$\Gamma_L^{\rm in} = \Gamma f(\epsilon,T,\mu), \quad \Gamma_L^{\rm out} = \Gamma[1-f(\epsilon,T,\mu)] \quad (2)$$

$$\Gamma_R^{\rm in} = \Gamma f(\epsilon,T_R,\mu_R), \quad \Gamma_R^{\rm out} = \Gamma[1-f(\epsilon,T_R,\mu_R)]. \quad (3)$$

The master equation in Eq. (1) is valid in the weak-coupling regime when $\Gamma \ll T$. Average particle and heat currents, denoted by $\langle I_{\rm QD}^{(L/R)}\rangle$ and $\langle \dot{Q}_{\rm QD}^{(L/R)}\rangle$, respectively, flowing from the QD into the finite reservoir (L) and infinite reservoir (R), can be expressed as

$$\langle I_{\rm QD}^{(L/R)}\rangle = p_1\Gamma_{L/R}^{\rm out} - p_0\Gamma_{L/R}^{\rm in}, \quad (4)$$

$$\langle \dot{Q}_{\rm QD}^{(L/R)}\rangle = (\epsilon-\mu)\langle I_{\rm QD}^{(L/R)}\rangle. \quad (5)$$

Furthermore, we consider linear response equations to describe transport between the infinite and finite reservoirs [21]. The corresponding particle and heat currents are given by

$$\langle I_{\rm inf}\rangle = \sigma\Delta\mu, \quad \langle \dot{Q}_{\rm inf}\rangle = \frac{\pi^2\bar{T}\sigma}{3}\Delta T + \bar{\mu}\sigma\Delta\mu, \quad (6)$$

where $\bar{\mu} = (\mu_L+\mu)/2$ and $\bar{T} = (T_L+T)/2$ are the average chemical potential and temperature, and $\Delta\mu = \mu_L - \mu$ and $\Delta T = T_L - T$ are chemical potential and temperature differences. These expressions assume energy-independent transmission between the finite and infinite electron reservoirs, and are valid when the electrical conductance $\sigma$ is much larger than $\Delta\mu$ and $\Delta T$. In the Supplemental Material (SM) [36] (see also Refs. [37–39] therein), we provide a detailed analysis of their regime of validity using the Landauer-Büttiker formalism.

Finally, the exchange of heat between the finite electronic reservoir and the phonon bath is expressed as

$$\langle \dot{Q}\rangle = -\Sigma\left(T^n - T_{\rm ph}^n\right), \quad (7)$$

where $T_{\rm ph}$ is the temperature of the phonon bath and $\Sigma$ accounts for the phonon-electron interaction. Equation (7) is valid when we only consider a single phonon mode with a well-defined temperature $T_{\rm ph}$, and is valid to first order in $\Sigma$. Here, we only consider a single phonon mode with a well-defined temperature $T_{\rm ph}$. The extension to multiple phonon modes is, however, straightforward within our framework. The exponent $n$ takes different values depending on the system. Usually, $n=5$ for normal bulk metals [31,40], but other values are possible for dimensionally restricted electron gases [16,41–44].

From here on, we write $\langle I_{\rm QD}\rangle = \langle I_{\rm QD}^L\rangle$ and $\langle \dot{Q}_{\rm QD}\rangle = \langle \dot{Q}_{\rm QD}^L\rangle$ to ease the notation. The time evolution of the finite reservoir's chemical potential and temperature will depend on particle and heat currents as [21]

$$\dot{\mu} = \frac{1}{\nu_0}(\langle I_{\rm QD}\rangle + \langle I_{\rm inf}\rangle), \quad (8)$$

$$\dot{T} = \frac{1}{C_{\rm el}}(\langle \dot{Q}_{\rm QD}\rangle + \langle \dot{Q}_{\rm inf}\rangle + \langle \dot{Q}_{\rm ph}\rangle), \quad (9)$$

where $\nu_0$ is the density of states of the electrons (taken to be energy independent for simplicity), and $C_{\rm el} = \nu_0\pi^2 T/3$ is the specific heat of a free-electron gas. At the nonequilibrium stationary state (NESS), we have that $\dot{\mu} = \dot{T} = 0$. From now on, $T$ and $\mu$ will denote fixed, *stationary* temperature and

chemical potential of the finite reservoir, which can be found by self-consistently solving the coupled equations for the currents presented above.

The finite reservoir's NESS temperature and chemical potential depend on how strongly the finite reservoir couples to the infinite reservoir, the QD, and the phonon reservoir. In the following, we define the dimensionless quantity $\zeta = \sigma T_L/\Gamma$, representing the coupling strength of the finite reservoir to the infinite electron reservoir relative to its coupling to the QD. We also define $\xi = \Sigma T_{\rm ph}^n/\sigma T_L^2$, which captures the relative coupling strength of the finite reservoir to the phonon versus the electron reservoir. To make progress analytically, we assume that $\zeta \gg 1$ and $\xi \gg 1$, which describes the regime of a large, but still finite, reservoir [21] whose temperature is significantly influenced by the phonon bath. With these approximations, we can write $T = T_{\rm ph} + \Delta T$ and $\mu = \mu_L + \Delta\mu$, with $\Delta T/T_{\rm ph} \ll 1$ and $\Delta\mu/\mu_L \ll 1$ given by

$$\Delta\mu \approx -\frac{V_b}{\sigma}G, \quad \Delta T \approx \frac{\pi^2 T_{\rm ph}}{6n\xi}\left(1 - \frac{T_{\rm ph}^2}{T_L^2}\right), \tag{10}$$

where $G$ is the conductivity of transport through the QD. See the SM [36] for the detailed derivation and justification of the expressions in Eq. (10). The SM also provides an analysis of the contrasting regime in which $\xi \ll 1$ (ultraweak coupling to the phonon reservoir), but this yields substantially reduced thermometric sensitivity so we focus on the case of $\xi \gg 1$ from here on.

A few remarks about (10) are in order. We first note that $\Delta\mu$ is insensitive to the phonon temperature. This results from the fact that the phonon temperature enters (8) indirectly, through $T$. Instead, the change in $\mu$ is dictated by the relation between the tunneling strength into the QD and the infinite reservoir. On the other hand, $\Delta T$ is inversely proportional to the relative strength $\xi$.

*Estimation theory*. Given a sequence of measurement outcomes, $\mathbf{x} = \{x_1, x_2, \ldots, x_N\}$, an estimate of the phonon temperature can be obtained by employing an estimator, which is a function of the measurement data $\mathbf{x}$. In particular, *unbiased* estimators, $\check{T}_{\rm ph}(\mathbf{x})$, satisfy the property that their expected values, taken over all possible measurement records, correspond to the true value of the parameter, $\langle \check{T}_{\rm ph}(\mathbf{x})\rangle = T_{\rm ph}$. The precision of the phonon temperature estimation is captured by the variance of $\check{T}_{\rm ph}(\mathbf{x})$, which is bounded by the Cramér-Rao bound [45,46] as $\mathrm{Var}[\check{T}_{\rm ph}(\mathbf{x})] \geqslant 1/F(T_{\rm ph})$, where $F(T_{\rm ph})$ is the Fisher information [47]

$$F(T_{\rm ph}) = \sum_{\mathbf{x}} P(\mathbf{x})\left[\frac{\partial}{\partial T_{\rm ph}}\ln P(\mathbf{x})\right]^2. \tag{11}$$

Here, $P(\mathbf{x})$ is the $T_{\rm ph}$-dependent probability to obtain the measurement data $\mathbf{x}$.

*Strategy I*. We first consider continuously measuring the system, as it evolves under Eq. (1). In this case, measurement outcomes are, in general, correlated with each other [48]. A measurement record is, in this way, constituted of data points characterizing a given *trajectory*. For example, trajectories can be constructed by keeping track of the sequence of stochastic jumps of electrons tunnel in and out of the QD, $\mathbf{x} = \{x_1, x_2, \ldots, x_N\}$, during the time interval $0 \leqslant t \leqslant \tau$.

In this case, for a sufficiently large $\tau$, the Fisher information can be expressed as [49]

$$F_{\rm I}(T_{\rm ph}) = \left[\left(\partial_{T_{\rm ph}}\Gamma_L^{\rm in}\right)^2\frac{p_0^{\rm ss}}{\Gamma_L^{\rm in}} + \left(\partial_{T_{\rm ph}}\Gamma_L^{\rm out}\right)^2\frac{p_1^{\rm ss}}{\Gamma_L^{\rm out}}\right]\tau, \tag{12}$$

where $p_1^{\rm ss} = (f + f_R)/2$ and $p_0^{\rm ss} = 1 - p_1^{\rm ss}$ are stationary probabilities. We note that $F_{\rm I}$ depends only on the rates describing the coupling to the finite reservoir, $\Gamma_L^{\rm in}, \Gamma_L^{\rm out}$, as the derivatives of $\Gamma_R^{\rm in}, \Gamma_R^{\rm out}$ with respect to the phonon temperature are zero. In this way, the sensitivity is entirely determined by the exchange of quanta with the finite reservoir. In the SM [36], by considering the approximations in (10), we show that $F_{\rm I}$ can be approximated as

$$F_{\rm I}(T_{\rm ph}) \approx \chi_e\chi_{\rm ph}\left[\frac{\langle N_{\rm in}\rangle}{f^2} + \frac{\langle N_{\rm out}\rangle}{\bar{f}^2}\right], \tag{13}$$

where $f = f(\epsilon, T, \mu)$ and $\bar{f} = 1 - f(\epsilon, T, \mu)$, while $\langle N_{\rm in}\rangle = p_0^{\rm ss}\Gamma_L^{\rm in}\tau$ and $\langle N_{\rm out}\rangle = p_1^{\rm ss}\Gamma_L^{\rm out}\tau$. Additionally, we have that

$$\chi_e \equiv \left(\frac{\partial f}{\partial T}\right)^2 = \frac{(\epsilon-\mu)^2}{16T^4\cosh^4\left(\frac{\epsilon-\mu}{2T}\right)}, \tag{14}$$

$$\chi_{\rm ph} \equiv \left(\frac{\partial T}{\partial T_{\rm ph}}\right)^2 = \left[1 + \frac{\pi^2}{6n\xi}\left((1-n) + \frac{T_{\rm ph}^2}{T_L^2}(n-3)\right)\right]^2. \tag{15}$$

The expression in Eq. (13) is particularly insightful, as each of the three multiplicative factors captures distinct contributions to the phonon temperature sensitivity, as explained in the following. The first factor, $\chi_e$, quantifies the sensitivity of the finite reservoir's Fermi-Dirac occupation, $f(\epsilon, T, \mu)$, to changes in its temperature $T$. The second factor, $\chi_{\rm ph}$, measures how $T$ changes with the phonon temperature. Altogether, the product $\chi_e\chi_{\rm ph}$ weights the Fisher information with the sensitivity of the finite reservoir to the phonon temperature. In this sense, we show that the finite reservoir temperature becomes independent of $T_{\rm ph}$ when $\xi \to 0$ and $\zeta \to 0$. This means that $\chi_{\rm ph}$ vanishes in the limit of an infinitely large electronic reservoir, which implies zero sensitivity (see the SM [36]). Finally, the last factor is expressed in terms of the expected value of the number of tunneling events into (out) the QD from (into) the finite reservoir during the measuring time $\tau$, $\langle N_{\rm in}\rangle$ ($\langle N_{\rm out}\rangle$).

To put our result in Eq. (12) into perspective, we consider the upper bound on the Fisher information, namely the *quantum Fisher information* [50], derived by Gammelmark and Mølmer [51] for measurements on the global system (i.e., system and environment) during a certain time $\tau$. Specifically, they obtained an analytical expression for the Fisher information corresponding to the optimal measurement on the global system, out of all possible quantum measurements. This result therefore corresponds to the maximum precision achievable by measuring the global system for a sufficiently long time (see the SM [36] for details).

In the SM [36], we show that, in the long-time limit, the Fisher information for jump trajectories equals the upper bound derived in Ref. [51] for any classical rate equation. We can therefore conclude that, for very large $\tau$, monitoring jumps corresponds to the best possible precision.

*Strategy II*. We will now consider measuring the net charge $N$ transferred from the QD into the right reservoir during the time $\tau$. Such a measurement can be performed by integrating the dc current measured by an ammeter over a time window $\tau$, and can be modeled theoretically as a two-point measurement of the number of electrons in a given reservoir [52]. For large $\tau$, the average and fluctuations of $N$ increase linearly with time, i.e., $\langle N\rangle = \tau\langle I_{\mathrm{QD}}\rangle$ and $\mathrm{Var}(N) = \tau\langle\langle I^2_{\mathrm{QD}}\rangle\rangle$, with $\langle\langle I^2_{\mathrm{QD}}\rangle\rangle$ being the diffusion coefficient [53]. Given this, the asymptotic Fisher information for such a current measurement can be expressed as $F(T_{\mathrm{ph}}) = \tau(\partial_{T_{\mathrm{ph}}}\langle I_{\mathrm{QD}}\rangle)^2/\langle\langle I^2_{\mathrm{QD}}\rangle\rangle$ [8].

In our case, the average current reads $\langle I_{\mathrm{QD}}\rangle = \Gamma(f - f_R)/2$. As we assume that the finite reservoir is large enough, i.e., $\zeta \gg 1$, we neglect temperature fluctuations in the stationary state. In this way, the calculation of the diffusion coefficient gives (see the SM [36] for details)

$$\langle\langle I^2_{\mathrm{QD}}\rangle\rangle = \Gamma\left[\frac{f\bar{f} + f_R\bar{f}_R}{2} + \frac{(f_R - f)^2}{4}\right]. \tag{16}$$

Using (10), we obtain the following expression for the Fisher information,

$$F_{\mathrm{II}}(T_{\mathrm{ph}}) \approx \chi_e\chi_{\mathrm{ph}}\frac{\Gamma\tau}{(f + f_R)(\bar{f} + \bar{f}_R)}. \tag{17}$$

We can immediately see that the first two factors in Eq. (17), $\chi_e$ and $\chi_{\mathrm{ph}}$, are the same as in Eq. (13). The third factor in Eq. (17) quantifies how much information about the phonon temperature can be extracted from the total current flowing through the QD.

*Strategy III*. Lastly, we consider *repeated measurements* on the system. The protocol is as follows. After the QD evolve into the NESS, a measurement of the QD occupation is performed. Then, the system is again allowed to evolve for a sufficiently long time, so that it relaxes back into the NESS, and a new measurement of the QD occupation is realized. This procedure is repeated $N$ times, thereby giving rise to $N$ independent measurement outcomes. In this context, the Fisher information for the measurement of the QD occupation can be expressed as $F_{\mathrm{III}}(T_{\mathrm{ph}}) = (\partial_{T_{\mathrm{ph}}}\langle\hat{n}\rangle)^2/\langle\langle\hat{n}^2\rangle\rangle$, where $\langle\hat{n}\rangle = p^{\mathrm{ss}}_1$ is the average occupation of the QD, while its fluctuations are given by

$$\langle\langle\hat{n}^2\rangle\rangle = \langle\hat{n}^2\rangle - \langle\hat{n}\rangle^2 = \frac{f\bar{f} + f_R\bar{f}_R}{2} + \frac{(f_R - f)^2}{4}, \tag{18}$$

where we used that $\langle\hat{n}^2\rangle = \langle\hat{n}\rangle$. Using (10), we get

$$F_{\mathrm{III}}(T_{\mathrm{ph}}) \approx \chi_e\chi_{\mathrm{ph}}\frac{1}{(f + f_R)(\bar{f} + \bar{f}_R)}. \tag{19}$$

We note that the Fisher information for a single occupation measurement in Eq. (19) only differs from $F_{\mathrm{II}}$ in Eq. (17) by a factor of $\Gamma\tau$. If we now express $N = \tau/\tau_M$, where $\tau_M$ is the time interval between measurements, we have that

$$NF_{\mathrm{III}} = \frac{F_{\mathrm{II}}}{\Gamma\tau_M}. \tag{20}$$

In order to ensure that the system has reached its NESS before performing a new measurement of the occupation, $\tau_M$ must be significantly larger than the relaxation timescale of the system, $\tau_{\mathrm{rel}}$. The latter is determined by the nonzero eigenvalue of the rate matrix $\mathcal{W}$ in Eq. (1), and is given by $\tau_{\mathrm{rel}} = 1/2\Gamma$. Thus,

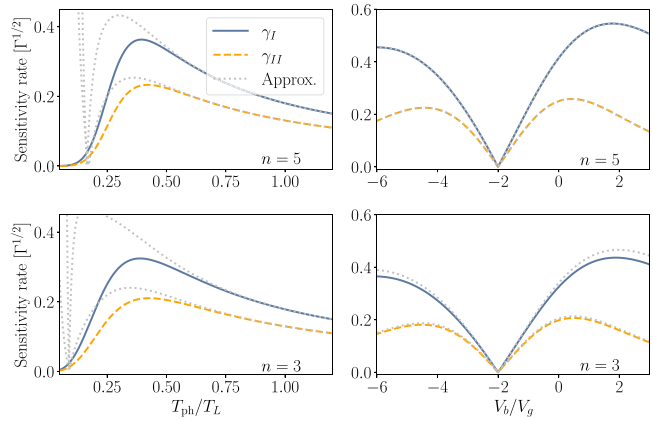



FIG. 2. Sensitivity rate of the three thermometry schemes as a function of (left column) phonon temperature and (right column) bias voltage. The top row has electron-phonon coupling with an exponent $n = 5$, while the bottom row has $n = 3$. The parameters used are $T_L = T_R = 10\Gamma$, $V_b = 40\Gamma$, $\sigma = 300\Gamma/T_L$, and $V_g = -10\Gamma$. When $n = 5$, we use $\Sigma = 1000\sigma/T_L^3$, and when $n = 3$, we use $\Sigma = 100\sigma/T_L$. In the right column, we set the phonon temperature to $T_{\mathrm{ph}} = 8\Gamma$.

if we fix the time between measurements to be $\tau_M = 2\eta\tau_{\mathrm{rel}}$ for some constant factor $\eta > 1$, then we find $NF_{\mathrm{III}} = F_{\mathrm{II}}/\eta$, i.e., the total Fisher information for strategy III is less than for strategy II. Finally, we note that the Fisher information in strategies II and III is only proportional if the coupling strength $\Gamma$ with the left and right reservoirs is the same.

*Thermometric precision*. The Fisher information in Eqs. (13) and (17) increase linearly with time. In order to compare the thermometric performance of the current-based strategies I and II, we define the sensitivity rate as

$$\gamma_l^2 = \frac{T^2_{\mathrm{ph}}F_l}{\tau}, \tag{21}$$

where $l = \mathrm{I}, \mathrm{II}$ and $F_l$ is the corresponding Fisher information. We evaluate the sensitivity rates numerically, which are plotted in Fig. 2 for strategies I (solid blue lines) and II (dashed orange lines) as a function of the phonon temperature, $T_{\mathrm{ph}}/T_L$ (left column) and bias voltage $V_b/V_g$ (right column). They are shown for phonon-electron coupling models for which $n = 5$ (top row) and $n = 3$ (bottom row). We also plot the approximations in Eqs. (13) and (17) (gray dotted lines). In all cases, we see that strategy I, where the sequence of jumps is monitored, significantly outperforms strategy II. This is expected, since Eq. (12) corresponds to the optimal measurement performed on the global system during the time $\tau$.

In the left column of Fig. 2, we see that the sensitivity rates display a nonmonotonic behavior as a function of $T_{\mathrm{ph}}$. The approximations agree with the numerical results for $T_{\mathrm{ph}}$ large enough, so that $\xi \gg 1$. We also note that we get a significant difference in the value of sensitivity rates for different values of $n$. More specifically, the sensitivity rate is always higher for $n = 5$ than for $n = 3$. This can be understood as $\xi \propto T^n_{\mathrm{ph}}$, i.e., phonons couple more strongly to the finite reservoir for $n = 5$ than for $n = 3$. In the right column of Fig. 2, both $\gamma_{\mathrm{I}}$ and $\gamma_{\mathrm{II}}$ vanish at the point where the chemical potential of

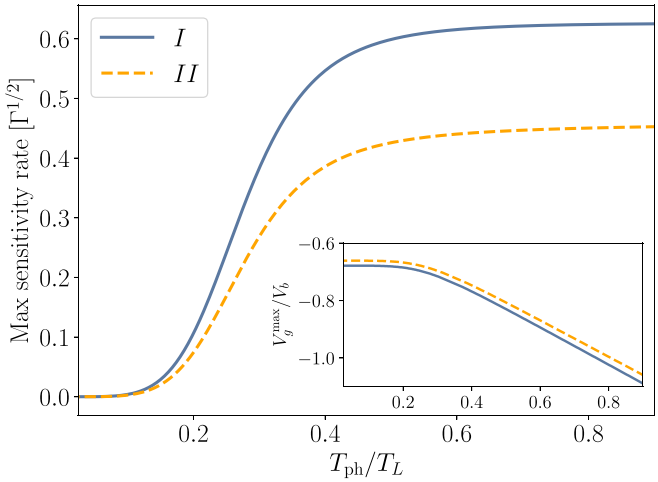



FIG. 3. Optimized sensitivity rate over gate voltage as the phonon temperature $T_{\rm ph}$ is varied. The inset shows the corresponding optimal bias voltage. The parameters used are $n = 5$, $T_L = T_R = 10\Gamma$, $V_b = 40\Gamma$, $\sigma = 300\Gamma/T_L$, and $\Sigma = 1000\sigma/T_L^3$. For these parameters, we have that $\zeta = 300$, and $\xi \gg 1$, provided the phonon temperature is sufficiently large, i.e., $T_{\rm ph} \gtrsim T_L/3$.

the finite reservoir is equal to the QD level energy, $\mu = \epsilon$. This is because $\chi_e = 0$ at this point, as the tunneling rates become independent of finite reservoir temperature. We also see that the sensitivity rates increase linearly from the point where $\mu = \epsilon$, in agreement with Eqs. (13) and (17). Overall, we see that the numerically calculated sensitivities agree with the approximations to a remarkable degree in the considered range for the voltage bias.

As we have seen, Fig. 2 demonstrates the existence of optimal current-based sensing of phonon temperature for any set of parameters. We further numerically investigate this by considering the optimisation of sensitivity rates over the experimentally tunable gate voltage, $V_g$,

$$\gamma_l^{\max} = \max_{V_g} \gamma_l, \tag{22}$$

for a fixed value of phonon temperature. We denote the gate voltage that maximizes the sensitivity rate by $V_g^{\max}$. The result of the optimisation is shown in Fig. 3 for both strategies I and II. We see that, for $T_{\rm ph} \gtrsim T_L/3$, a very favorable and robust estimation regime is achieved. The inset shows the corresponding optimal gate voltage for both strategies. These results can guide experimentalists to implement optimal phonon temperature sensing schemes by tuning the gate voltage.

*Conclusion*. We introduced an approach harnessing finite reservoirs for current-based phonon temperature estimation in the long-time limit. By showing that the Fisher information for jump trajectories corresponds to the quantum Fisher information for any classical rate equation, we were able to demonstrate that monitoring the sequence of electron jumps between the QD system and the finite reservoir (strategy I) enables the best possible current-based sensitivity. We also investigated the sensitivities of measuring the total charge transferred (strategy II) and the QD occupation (strategy III). For large but still finite reservoirs, we derived analytical expressions for the Fisher information in strategies I, II, and III. These expressions clearly capture the finite reservoir's thermometric contribution via common multiplicative factors. Furthermore, we demonstrate optimal precision within current strategies I and II by tuning the gate voltage.

In most experimental scenarios, it will be easiest to use the estimation scheme II, which requires only a simple dc current measurement. Strategy III can be realized using fast real-time detection of the QD charge state, e.g., via radio-frequency reflectometry [54]. However, as we have shown, this does not give any significant advantage in our setting, since strategy II yields a higher rate of precision gain once the time between measurements in strategy III is accounted for. Strategy I is theoretically optimal but also the most challenging to realize, as it requires resolving each individual exchange of charge between the QD and the finite reservoir. Such detection of jumps mediated by a specific reservoir is not out of the question in more complex nonequilibrium setups, e.g., as demonstrated recently using real-time charge detection on a double-quantum-dot system in the high-bias, Coulomb blockade regime [55].

In conclusion, our results show how finite reservoirs can be harnessed for metrology in nonequilibrium steady states. While we focus on an electronic transport setup, our results serve as a basis for the investigation of how finite reservoirs can be harnessed for current-based parameter estimation in other scenarios, such as superconducting qubits coupled to bosonic environments [12,13].

*Acknowledgments*. We gratefully acknowledge discussions with G. T. Landi regarding the QFI for classical rate equations. We also thank L. Banszerus for insightful discussions. S.B. and M.T.M. acknowledge the financial support of the Royal Society and Research Ireland. M.T.M. is supported by a Royal Society University Research Fellowship. S.M. acknowledges financial support from Provincia Autonoma di Trento (PAT); from the Q@TN Initiative; from the National Quantum Science and Technology Institute through the PNRR MUR project under Grant No. PE0000023-NQSTI, co-funded by the European Union – NextGeneration EU. This project is co-funded by the European Union (Quantum Flagship project ASPECTS, Grant Agreement No. 101080167) and UK Research & Innovation (UKRI).

Views and opinions expressed are however those of the authors only and do not necessarily reflect those of the European Union, Research Executive Agency or UKRI. Neither the European Union nor UKRI can be held responsible for them.

*Data availability*. There are no publicly available research data or software supporting this manuscript. Requests for further information or data should be sent to the authors.

[1] T. Beechem, S. Graham, S. P. Kearney, L. M. Phinney, and J. R. Serrano, Invited article: Simultaneous mapping of temperature and stress in microdevices using micro-Raman spectroscopy, Rev. Sci. Instrum. **78**, 061301 (2007).

[2] T. Beechem, L. Yates, and S. Graham, Invited review article: Error and uncertainty in Raman thermal conductivity measurements, Rev. Sci. Instrum. **86**, 041101 (2015).
[3] S. Sandell, E. Chávez-Ángel, A. El Sachat, J. He, C. M. S. Torres, and J. Maire, Thermoreflectance techniques and Raman thermometry for thermal property characterization of nanostructures, J. Appl. Phys. **128**, 131101 (2020).
[4] P. P. Hofer, J. B. Brask, M. Perarnau-Llobet, and N. Brunner, Quantum thermal machine as a thermometer, Phys. Rev. Lett. **119**, 090603 (2017).
[5] D. Maradan, L. Casparis, T.-M. Liu, D. E. F. Biesinger, C. P. Scheller, D. M. Zumbühl, J. D. Zimmerman, and A. C. Gossard, GaAs quantum dot thermometry using direct transport and charge sensing, J. Low Temp. Phys. **175**, 784 (2014).
[6] J. Yang, C. Elouard, J. Splettstoesser, B. Sothmann, R. Sánchez, and A. N. Jordan, Thermal transistor and thermometer based on Coulomb-coupled conductors, Phys. Rev. B **100**, 045418 (2019).
[7] G. Mihailescu, A. Kiely, and A. K. Mitchell, Quantum sensing with nanoelectronics: Fisher information for an applied perturbation, arXiv:2406.18662.
[8] S. Khandelwal, G. T. Landi, G. Haack, and M. T. Mitchison, Current-based metrology with two-terminal mesoscopic conductors, Phys. Rev. B **112**, L161409 (2025).
[9] J. Boeyens, B. Annby-Andersson, P. Bakhshinezhad, G. Haack, M. Perarnau-Llobet, S. Nimmrichter, P. P. Potts, and M. Mehboudi, Probe thermometry with continuous measurements, New J. Phys. **25**, 123009 (2023).
[10] J. P. Pekola and B. Karimi, *Colloquium*: Quantum heat transport in condensed matter systems, Rev. Mod. Phys. **93**, 041001 (2021).
[11] B. Dutta, D. Majidi, N. W. Talarico, N. Lo Gullo, H. Courtois, and C. B. Winkelmann, Single-quantum-dot heat valve, Phys. Rev. Lett. **125**, 237701 (2020).
[12] M. Spiecker, P. Paluch, N. Gosling, N. Drucker, S. Matityahu, D. Gusenkova, S. Günzler, D. Rieger, I. Takmakov, F. Valenti, P. Winkel, R. Gebauer, O. Sander, G. Catelani, A. Shnirman, A. V. Ustinov, W. Wernsdorfer, Y. Cohen, and I. M. Pop, Two-level system hyperpolarization using a quantum Szilard engine, Nat. Phys. **19**, 1320 (2023).
[13] M. Spiecker, A. I. Pavlov, A. Shnirman, and I. M. Pop, Solomon equationsfor qubit and two-level systems: Insights into non-Poissonian quantum jumps, Phys. Rev. A **109**, 052218 (2024).
[14] V. Champain, V. Schmitt, B. Bertrand, H. Niebojewski, R. Maurand, X. Jehl, C. B. Winkelmann, S. De Franceschi, and B. Brun, Real-time millikelvin thermometry in a semiconductor-qubit architecture, Phys. Rev. Appl. **21**, 064039 (2024).
[15] H. Pothier, S. Guéron, N. O. Birge, D. Esteve, and M. H. Devoret, Energy distribution function of quasiparticles in mesoscopic wires, Phys. Rev. Lett. **79**, 3490 (1997).
[16] D. R. Schmidt, R. J. Schoelkopf, and A. N. Cleland, Photon-mediated thermal relaxation of electrons in nanostructures, Phys. Rev. Lett. **93**, 045901 (2004).
[17] F. Gallego-Marcos, G. Platero, C. Nietner, G. Schaller, and T. Brandes, Nonequilibrium relaxation transport of ultracold atoms, Phys. Rev. A **90**, 033614 (2014).
[18] G. Schaller, C. Nietner, and T. Brandes, Relaxation dynamics of meso-reservoirs, New J. Phys. **16**, 125011 (2014).
[19] C. Grenier, C. Kollath, and A. Georges, Thermoelectric transport and Peltier cooling of cold atomic gases, C. R. Phys. **17**, 1161 (2016).
[20] G. Amato, H.-P. Breuer, S. Wimberger, A. Rodríguez, and A. Buchleitner, Noninteracting many-particle quantum transport between finite reservoirs, Phys. Rev. A **102**, 022207 (2020).
[21] S. Matern, S. V. Moreira, P. Samuelsson, and M. Leijnse, Thermoelectric cooling of a finite reservoir coupled to a quantum dot, Phys. Rev. B **110**, 205423 (2024).
[22] P. Strasberg and A. Winter, First and second law of quantum thermodynamics: A consistent derivation based on a microscopic definition of entropy, PRX Quantum **2**, 030202 (2021).
[23] A. Riera-Campeny, A. Sanpera, and P. Strasberg, Quantum systems correlated with a finite bath: Nonequilibrium dynamics and thermodynamics, PRX Quantum **2**, 010340 (2021).
[24] A. Riera-Campeny, A. Sanpera, and P. Strasberg, Open quantum systems coupled to finite baths: A hierarchy of master equations, Phys. Rev. E **105**, 054119 (2022).
[25] C. Elouard and C. Lombard Latune, Extending the laws of thermodynamics for arbitrary autonomous quantum systems, PRX Quantum **4**, 020309 (2023).
[26] S. V. Moreira, P. Samuelsson, and P. P. Potts, Stochastic thermodynamics of a quantum dot coupled to a finite-size reservoir, Phys. Rev. Lett. **131**, 220405 (2023).
[27] H. Yuan, Y.-H. Ma, and C. P. Sun, Optimizing thermodynamic cycles with two finite-sized reservoirs, Phys. Rev. E **105**, L022101 (2022).
[28] P. Strasberg, M. G. Díaz, and A. Riera-Campeny, Clausius inequality for finite baths reveals universal efficiency improvements, Phys. Rev. E **104**, L022103 (2021).
[29] I. N. Mamede, S. V. Moreira, M. T. Mitchison, and C. E. Fiore, Steady-state heat engines driven by finite reservoirs, Phys. Rev. E **113**, 014115 (2026).
[30] B. Donvil and J. Ankerhold, Apparent heating due to imperfect calorimetric measurements, J. Phys. A: Math. Theor. **55**, 225303 (2022).
[31] F. Brange, P. Samuelsson, B. Karimi, and J. P. Pekola, Nanoscale quantum calorimetry with electronic temperature fluctuations, Phys. Rev. B **98**, 205414 (2018).
[32] B. Karimi, F. Brange, P. Samuelsson, and J. P. Pekola, Reaching the ultimate energy resolution of a quantum detector, Nat. Commun. **11**, 367 (2020).
[33] T. L. van den Berg, F. Brange, and P. Samuelsson, Energy and temperature fluctuations in the single electron box, New J. Phys. **17**, 075012 (2015).
[34] G.-L. Ingold and Y. V. Nazarov, Charge tunneling rates in ultrasmall junctions, in *Single Charge Tunneling*, edited by H. Grabert and M. H. Devoret (Springer, New York, 1992), Chap. 2, pp. 21–107.
[35] V. N. Golovach, X. Jehl, M. Houzet, M. Pierre, B. Roche, M. Sanquer, and L. I. Glazman, Single-dopant resonance in a single-electron transistor, Phys. Rev. B **83**, 075401 (2011).
[36] See Supplemental Material at http://link.aps.org/supplemental/10.1103/7jl4-jryx for derivations of the linear response equations for the transport between the infinite and finite reservoirs, linear response equations for the transport between the infinite and finite reservoirs, and transport expressions between the finite reservoir and the QD. It also contains the investigation of the regimes for which $\xi \ll 1$ and $\xi \gg 1$, the derivation of the quantum Fisher information for a rate equation in the long-time

limit, as well as the analytical expressions for current-based Fisher information in the main text, $F_{\mathrm{I}}$ and $F_{\mathrm{II}}$.

[37] G. Lindblad, On the generators of quantum dynamical semigroups, Commun. Math. Phys. **48**, 119 (1976).

[38] V. Gorini, A. Kossakowski, and E. C. G. Sudarshan, Completely positive dynamical semigroups of $N$-level systems, J. Math. Phys. **17**, 821 (1976).

[39] K. Yamamoto and N. Hatano, Thermodynamics of the mesoscopic thermoelectric heat engine beyond the linear-response regime, Phys. Rev. E **92**, 042165 (2015).

[40] J. P. Pekola and B. Karimi, Quantum noise of electron–phonon heat current, J. Low Temp. Phys. **191**, 373 (2018).

[41] E. Chow, H. P. Wei, S. M. Girvin, and M. Shayegan, Phonon emission from a 2D electron gas: Evidence of transition to the hydrodynamic regime, Phys. Rev. Lett. **77**, 1143 (1996).

[42] F. Giazotto, T. T. Heikkilä, A. Luukanen, A. M. Savin, and J. P. Pekola, Opportunities for mesoscopics in thermometry and refrigeration: Physics and applications, Rev. Mod. Phys. **78**, 217 (2006).

[43] M. Wiesner, K. Koski, A. Laitinen, J. Manninen, A. A. Zyuzin, and P. Hakonen, Electron–phonon coupling in copper intercalated $Bi_2Se_3$, Sci. Rep. **12**, 12097 (2022).

[44] P. Singh, M. Seong, and S. Sinha, Detailed consideration of the electron-phonon thermal conductance at metal-dielectric interfaces, Appl. Phys. Lett. **102**, 181906 (2013).

[45] H. Cramér, *Mathematical Methods of Statistics* (Princeton University Press, Princeton, NJ, 1946).

[46] C. R. Rao, *Linear Statistical Inference and Its Applications* (Wiley, New York, 1973).

[47] S. M. Kay, *Fundamentals of Statistical Signal Processing. 1: Estimation Theory*, 20th ed. (Prentice Hall PTR, Upper Saddle River, NJ, 2013).

[48] M. Radaelli, G. T. Landi, K. Modi, and F. C. Binder, Fisher information of correlated stochastic processes, New J. Phys. **25**, 053037 (2023).

[49] J. A. Smiga, M. Radaelli, F. C. Binder, and G. T. Landi, Stochastic metrology and the empirical distribution, Phys. Rev. Res. **5**, 033150 (2023).

[50] M. G. A. Paris, Quantum estimation for quantum technology, Int. J. Quantum Inf. **07**, 125 (2009).

[51] S. Gammelmark and K. Mølmer, Fisher information and the quantum Cramér-Rao sensitivity limit of continuous measurements, Phys. Rev. Lett. **112**, 170401 (2014).

[52] M. Esposito, U. Harbola, and S. Mukamel, Nonequilibrium fluctuations, fluctuation theorems, and counting statistics in quantum systems, Rev. Mod. Phys. **81**, 1665 (2009).

[53] G. T. Landi, M. J. Kewming, M. T. Mitchison, and P. P. Potts, Current fluctuations in open quantum systems: Bridging the gap between quantum continuous measurements and full counting statistics, PRX Quantum **5**, 020201 (2024).

[54] F. Vigneau, F. Fedele, A. Chatterjee, D. Reilly, F. Kuemmeth, M. Fernando Gonzalez-Zalba, E. Laird, and N. Ares, Probing quantum devices with radio-frequency reflectometry, Appl. Phys. Rev. **10**, 021305 (2023).

[55] V. Wadhia, F. Meier, F. Fedele, R. Silva, N. Nurgalieva, D. L. Craig, D. Jirovec, J. Saez-Mollejo, A. Ballabio, D. Chrastina, G. Isella, M. Huber, M. T. Mitchison, P. Erker, and N. Ares, Entropic costs of extracting classical ticks from a quantum clock, Phys. Rev. Lett. **135**, 200407 (2025).